Astron. Astrophys. 336, L1–L4 (1998)

ASTRONOMY AND ASTROPHYSICS

LETTER

Letter to the Editor

Evidence for X-ray emission from the type Ic supernova 1994I

S. Immler, W. Pietsch, and B. Aschenbach

Max-Planck-Institut für Extraterrestrische Physik, Postfach 1603, D-85740 Garching, Germany

Received 19 May 1998 / Accepted 3 June 1998

Abstract. X-ray observations of the galaxy NGC 5194 (M 51) with the High Resolution Imager (HRI) onboard ROSAT were analysed to search for X-ray emission from the type Ic supernova 1994I. An X-ray source with a (0.1–2.4 keV) luminosity of 1.6×10^{38} erg s^{-1} is found at the position of SN 1994I, 79–85 days after the explosion. We believe this to be the first detection of X-ray emission from a type I SN. Assuming the emission arises from shocked circumstellar gas, deposited by the progenitor through non-conservative mass-transfer to a companion, we estimate a constant gas density of $\rho = 2 \times 10^5$ cm^{-3} $v_{16\,500}^{2/3}$ and a total mass of X-ray luminous gas of $M = 1 \times 10^{-3} M_\odot$ inside a sphere of radius 1.2×10^{16} cm. If the emission arises from the shocked stellar wind of the progenitor, heated by the outgoing wave, we derive a mass-loss rate prior to the outburst of $\dot{M} = 3.6 \times 10^{-6}\, M_\odot\,\mathrm{yr}^{-1}$, similar to mass-loss rates of other type I SNe, inferred from radio observations.

Key words: supernovae: general – supernovae: individual: SN 1994I – galaxies: individual: NGC 5194 (M 51) – X-rays: galaxies – X-rays: general

1. Introduction

Supernova 1994I in NGC 5194 (M 51) was independently discovered by four groups of observers on April 2, 1994 (Puckett et al. 1994), and was identified as a type Ic supernova (SN), resulting from the iron core collapse of a C+O star (cf. Schmidt et al. 1994; Clocchiatti et al. 1994; Nomoto et al. 1994). In this *Letter*, we adopt an assumed date of explosion of March 31, 1994 (Chandler et al. 1994). Multiwavelength follow-up observations indicated that, whereas the amount of ejected mass was very low, the circumstellar matter had a sufficiently high density to produce strong radio emission. SN 1994I is thus a promising target for X-ray investigation because of the expected X-ray emission due to the circumstellar matter interaction, once the expanding shell becomes optically thin (cf. Rupen et al. 1994; Filippenko et al. 1995; Baron et al. 1996; Richmond et al. 1996). Whereas X-ray emission from eight type II SNe has been established to date, no detections of type I SNe in X-rays are reported (cf. Schlegel 1995 for a review of X-ray observations of SNe to the year 1995; Fabian & Terlevich 1996; Lewin et al. 1996; Immler et al. 1998a for detections thereafter).

Send offprint requests to: S. Immler (e-mail: simmler@mpe.mpg.de)

2. Observations and data reduction

The galaxy pair NGC 5194/5 was observed with the High Resolution Imager (HRI) onboard ROSAT (Trümper 1983) in five separate pointings in Dec. 1991/Jan. 1992 (8.5 ks), May/June 1992 (8.8 ks), May 1994 (9.4 ks), June 1994 (36.3 ks) and Dec. 1997 (5.0 ks). Results from the 1991/92 observations are discussed in Ehle et al. (1995).

Eight point sources visible in the merged 68 ks observation were used to align each of the 33 different observation intervals (OBIs) with respect to the first. No offset is seen to exceed $5\farcs3$. To test the resulting attitude solution, we compared the positions of five point-like X-ray sources with possible optical counterparts suggested by the APM finding charts (Irwin et al. 1994). The resulting systematic error of the attitude solution was found to be $3\farcs2$. In order to reduce background contamination due to UV emission, cosmic rays, etc., only HRI raw channels 2–8 were used.

An 'image subtraction technique' was performed on the data to search for variable X-ray point sources within the galaxy. This technique is based on the creation of 'count rate images' over selected observation intervals, and subtracting these from the mean 'count rate image' over the complete 68 ks observation. The 36.3 ks observation from June 1994 was subdivided into two observation blocks of 6.4 ks and 29.9 ks integration time, respectively. The resulting six observation blocks used in the 'image subtraction technique' are listed in Table 1.

A Gaussian filter, corresponding to the on-axis HRI point-spread function (PSF) of $4\farcs7$, was applied to the count rate images, and each image was subtracted from the gauss-filtered count rate image of the complete observation. The resulting images show regions of variability only, their X-ray photon flux being enhanced or reduced when compared to their mean photon flux in the complete observation. A 'local detect' algorithm was applied to the images to search for variable point sources with variabilities exceeding a Gaussian significance of 3σ. The 'image subtraction technique' is very sensitive to variable X-ray sources, as the resulting image background consists only of

Table 1. ROSAT HRI observations of NGC 5194/5

Obs. no.		obs. time	date	day since explosion
1		8.5 ks	07/12/91 – 10/01/92	−798
2		8.8 ks	22/05/92 – 05/06/92	−679
3		9.4 ks	22/05/94 – 23/05/94	52
4		36.3 ks	18/06/94 – 24/06/94	79–85
4	4a	6.4 ks	18/06/94	79
	4b	29.9 ks	19/06/94 – 24/06/94	80–85
5		5.0 ks	26/12/97 – 30/12/97	1 368

Table 2. X-ray emission from the position of SN 1994I

Obs. no.		net counts	rate ($10^{-4}\,\frac{\mathrm{cts}}{\mathrm{s}}$)	F_x ($10^{-14}\,\frac{\mathrm{erg}}{\mathrm{cm^2\,s}}$)	L_x ($10^{38}\,\frac{\mathrm{erg}}{\mathrm{s}}$)
1		–	< 7.1	< 3.0	< 2.1
2		–	< 3.6	< 1.6	< 1.1
3		–	< 3.1	< 1.3	< 0.9
4		19 ± 6	5.2 ± 1.7	2.3 ± 0.7	1.6 ± 0.5
4	4a	7 ± 3	10.9 ± 3.1	4.7 ± 1.3	3.3 ± 0.9
	4b	12 ± 5	4.0 ± 1.7	1.7 ± 0.7	1.2 ± 0.5
5		–	< 8.4	< 3.7	< 2.5

background *fluctuation* since regions of constant X-ray emission are subtracted. The applied method is thus especially suited to searching for variable X-ray sources in regions of enhanced diffuse X-ray emission. The full details of the 'image subtraction technique' are described in Immler et al. (1998b).

3. Results

An X-ray point source is detected at the radio position of SN 1994I in the subtracted image from the 6.4 ks observation (no. 4a), together with seven variable X-ray sources within the inner $1' \times 1'$ of the galaxy (discussed in Immler et al. 1998b).

The offset between the X-ray source and the radio position of SN 1994I (R.A.^{2000} = $13^\mathrm{h}29^\mathrm{m}54\overset{\mathrm{s}}{.}07$, Dec.^{2000} = $+47°11'31\overset{''}{.}5$, Morrison & Argyle 1994) is $1\overset{''}{.}2$, well below the systematic error of the attitude solution ($3\overset{''}{.}2$). The source has a count rate excess of $(4.3 \pm 0.8) \times 10^{-4}$ cts s^{-1} in the 6.4 ks observation interval, compared to the complete observation. To confirm the existence of the source, a source detection algorithm was applied to images of pixel size $1''$ for the observation blocks listed in Table 1. The applied analysis procedures are described in Vogler & Pietsch (1996). Within the inner $1' \times 1'$ of the galaxy, two sources are detected in the observation blocks 4a and 4b, with a likelihood $L \geq 6$. While one source is located at the position of the optical nucleus of the galaxy, the other source coincides with the variable source found in the subtracted images at the position of SN 1994I. The source at the position of SN 1994I is detected with a likelihood of $L = 7.2$ (3.4σ) in the 6.4 ks observation (no. 4a) and with a likelihood of $L = 6.3$ (3.1σ) in the 29.9 ks observation (no. 4b). The corresponding net counts within an extraction circle of radius $5''$ are 7 ± 3 and 12 ± 5, respectively. Analysis of the complete 36.3 ks observation (no. 4) gives a total of 19 ± 6 net counts. No source is found at the position of SN 1994I for the remaining epochs at a 3σ confidence level, and 3σ upper limits (99.7% confidence level) were calculated.

Comparison of the HRI raw spectra of the source at the position of SN 1994I, the nuclear region of NGC 5194, and a large background region shows that photons from the background region are evenly distributed across the HRI raw channels 0–15, an expected result given the nature of the background (instrumental background, UV emission, weak galactic and extragalactic sources, cosmic rays, etc.). All source photons from the position of SN 1994I and photons from the nuclear region of NGC 5194, however, are contained in the HRI raw channels 1–8, the peak being located in channel 4.

Since SN 1994I is only $\sim 18''$ offset from the nucleus of NGC 5194, the contribution of emission from the extended bulge region to the emission of the source at the position of SN 1994I was estimated by constructing surface brightness profiles, centred on the X-ray peak emission of the galaxy. Three sectors were extracted, with radially binning of $1\overset{''}{.}75$. The sectors extend to $35''$ radius from the nucleus, having a width of $5''$ at the distance of SN 1994I. The middle sector is centred on the position of the SN, and the two adjacent sectors have been co-added. The location of the sectors are shown in the inset of Fig. 1 for the 6.4 ks observation (no. 4a). The inset image shows the X-ray contours from the inner $1' \times 1'$ nuclear region of NGC 5194. The contour levels are 1,1.5,2,3,4,5 and 6 in units of 1 count per detection cell (5.6×10^{-1} cts s^{-1} arcmin^{-2}). The position of the optical nucleus of NGC 5194 is at the origin of the sectors, while the radio position of the SN is indicated by a cross. Comparison of the surface brightness profiles of the sectors containing SN 1994I (solid line, labelled 'on') and the two adjacent sectors to either side (dashed line, 'off'), shows an excess of X-ray emission at the position of SN 1994I. The extended bulge emission component ('off') exceeds the PSF of the eight co-added point sources used for the boresight correction (dotted line, 'PSF'). The extent of the bulge emission, however, can only be observed to a distance of $\sim 12''$ from the nucleus of the galaxy. Hence, the contribution of the bulge emission to the source flux at the position of SN 1994I is negligible.

4. Discussion

The (0.1–2.4 keV) flux and luminosity of the source at the position of SN 1994I over observation block 4 (i.e. between days 79–85 after the outburst) are $F_\mathrm{x} = 2.3 \times 10^{-14}$ erg cm^{-2} s^{-1} and $L_\mathrm{x} = 1.6 \times 10^{38}$ erg s^{-1}, respectively, assuming a 5 keV thermal bremsstrahlung spectrum, a galactic hydrogen column of $N_\mathrm{H} = 1.3 \times 10^{20}$ cm^{-2} (Dickey & Lockman 1990) and a distance of 7.7 Mpc (Tully 1988). Assumption of a 1 keV thermal bremsstrahlung spectrum increases the source flux and luminosity by $\sim 5\%$. Fluxes and luminosities for observation bins

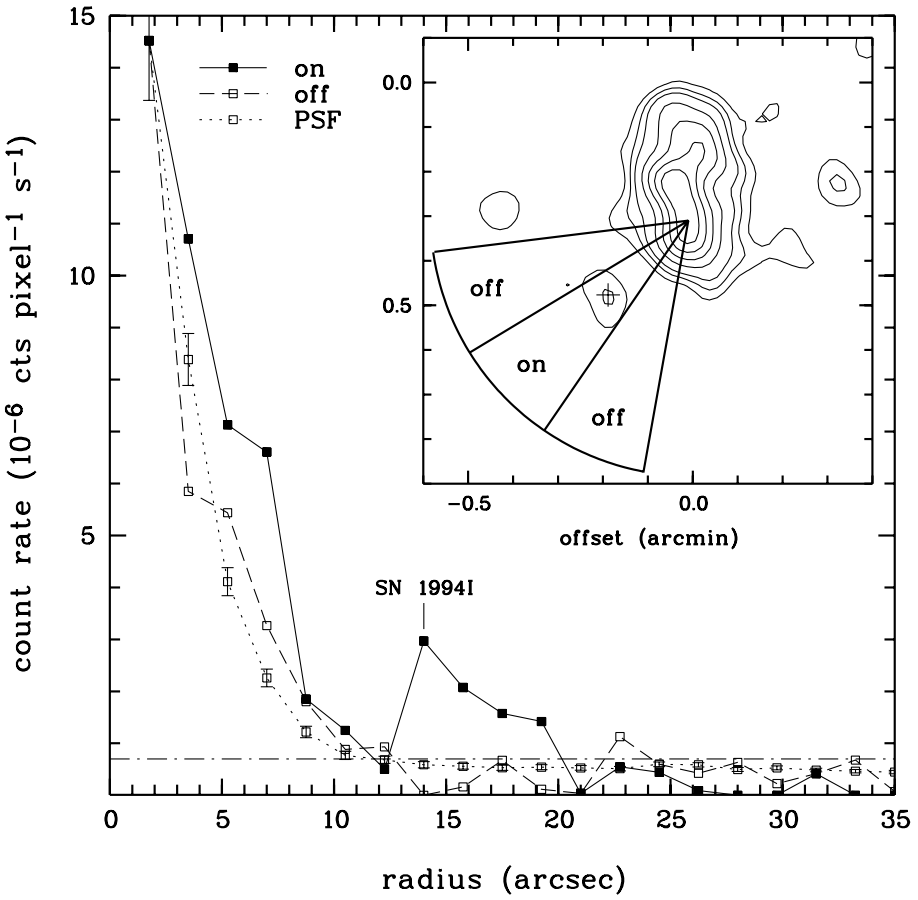

Fig. 1. Radial surface brightness profile of the X-ray emission, centred on the nucleus of NGC 5194. Photons were extracted from three sectors in the 6.4 ks observation (observation 4a in Table 1). The locations of the sectors are shown in the inset image, which gives a contour representation of the inner $1' \times 1'$ region X-ray emission from the 6.4 ks observation. The image was constructed with a pixel size of $1''$ and smoothed with a Gaussian filter of $4\farcs7$ FWHM. Contour levels are 1,1.5,2,3,4,5 and 6 in units of 1 count per detection cell (5.6×10^{-1} cts s^{-1} arcmin^{-2}). The position of the optical nucleus of NGC 5194 is at the origin of the sectors, the radio position of the SN 1994I is indicated by a cross. The solid line shows the radially-binned surface brightness profile of the X-ray emission from the center sector, containing SN 1994I ('on'). The dashed line gives the mean surface brightness profile of the emission in the two outer sectors ('off'). The dotted line gives the surface brightness profile of eight co-added point sources. The mean background level of 7×10^{-7} cts pixel^{-1} s^{-1} is indicated by the dot-dashed horizontal line.

4a and 4b are listed in Table 2, together with 3σ upper limits for the remaining epochs.

The chance probability of a background AGN, at the flux given above, being within $5''$ of the position of SN 1994I, is 3×10^{-5} (using the ROSAT Medium Sensitivity Survey; Hasinger et al. 1991). However, if we suppose that the seven variable sources detected with the 'image subtraction technique' are distributed randomly within the inner $1' \times 1'$ (excluding the source at the nucleus of the galaxy), we derive a probability of 15% that one of the sources accidentally falls within $5''$ of the position of the SN. It therefore should be stressed that we cannot be certain whether the X-ray source at the position of SN 1994I can be attributed to the supernova itself. The positional coincidence, however, is highly suggestive.

Two models have been proposed for the progenitor of SN 1994I, one by Woosley et al. (1995) and another by Nomoto et al. (1994). In the model presented by Woosley et al., the progenitor was in a close binary system and lost its outer envelope both by mass-transfer to the companion and by a strong stellar wind, leaving a C+O star, which exploded when its iron core collapsed. According to the circumstellar interaction model (cf. Chevalier 1984; Chevalier & Fransson 1994), the luminosity expected by thermal emission of the hot shocked wind is $L = 1 \times 10^{40} A^2 (t/10\,\mathrm{days})^{-1}$ erg s^{-1}, where A is defined by $\dot{M}/v_\mathrm{w} = 10^{-6}\,A\,(M_\odot\,\mathrm{yr}^{-1})/(\mathrm{km\,s}^{-1})$. Using our

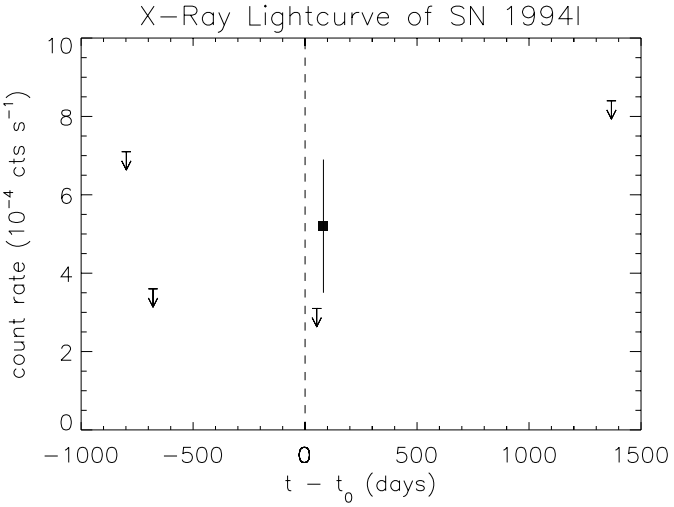

Fig. 2. X-ray lightcurve of SN 1994I. The data points correspond to the five HRI observations (cf. Table 2), time is given in days relative to the outburst of the SN (March 31, 1994). Arrows represent upper limits at a 3σ confidence level, the count rate error for observation 4 corresponds to a $\pm 1\sigma$ statistical error.

observed luminosity at $t = 82$ days (no. 4) and assuming a wind velocity of $v_\mathrm{w} = 10\,\mathrm{km\,s}^{-1}$, we derive a mass-loss rate of the progenitor of $\dot{M} = 3.6 \times 10^{-6} M_\odot\,\mathrm{yr}^{-1}$. This is typ-

ical of type I SNe, as inferred from radio observations (cf., e.g. SN 1983N, SN 1984L: $2 \times 10^{-6} M_\odot\,\mathrm{yr}^{-1}$, SN 1990B: $3 \times 10^{-6} M_\odot\,\mathrm{yr}^{-1}$, Weiler et al. 1993), whereas the mass-loss rate of type II SNe is more than an order of magnitude higher (cf., e.g. SN 1979C: $1 \times 10^{-4} M_\odot\,\mathrm{yr}^{-1}$, SN 1980K: $3 \times 10^{-5} M_\odot\,\mathrm{yr}^{-1}$, SN 1996J: $2 \times 10^{-4} M_\odot\,\mathrm{yr}^{-1}$, Weiler et al. 1993; SN 1988Z: $7 \times 10^{-5} M_\odot\,\mathrm{yr}^{-1}$, van Dyk et al. 1993). The only stringent upper limit to the X-ray flux of a type I SN (SN 1992A, type Ia) found to date implies a mass-loss rate of $\dot{M} < (2-3) \times 10^{-6} M_\odot\,\mathrm{yr}^{-1}$ (Schlegel & Petre 1993). However, as Chevalier (1998) pointed out in a recent paper, if synchrotron self-absorption is the dominant absorption mechanism, then it might not be possible to estimate the mass-loss rate using radio observations.

The second model, proposed by Nomoto et al. (1994), suggests that the progenitor of SN 1994I lost its envelope to the companion through two stages of non-conservative mass-transfer, which accounts for the presence of circumstellar matter. We can estimate the density and mass of the circumstellar matter by assuming that the observed X-ray emission on day 82 arises from the shocked circumstellar gas, heated by the outgoing wave. At this time, the SN ejecta had reached a distance of $r_{82} = 1.2 \times 10^{16}$ cm for an expansion velocity of $v_\mathrm{s} = 16\,500\ \mathrm{km\,s}^{-1}$ (Filippenko et al. 1995), well outside the orbit of the binary ($\sim 10^{13}$ cm). For $L_\mathrm{x} = \int \Gamma(T)(4\rho)^2 dV$ with a cooling function of $\Gamma(5\ \mathrm{keV}) = 3 \times 10^{-23}\ \mathrm{erg\,cm^3\,s^{-1}}$ (Raymond et al. 1976), we derive a constant density of $\rho = 2 \times 10^5\ \mathrm{cm}^{-3}\, v_{16\,500}^{2/3}$ (for a shell expansion velocity in units of $16\,500\ \mathrm{km\,s}^{-1}$) and a total mass of deposited X-ray luminous gas of $M = 1 \times 10^{-3} M_\odot$ inside a sphere of radius 1.2×10^{16} cm. On day 52, the expanding shell had reached a radius of $r_{52} = 7 \times 10^{15}$ cm. The expected L_x, normalized to that on day 82, is $4.1 \times 10^{37}\ \mathrm{erg\,s}^{-1}$ with $\rho = 2 \times 10^5\ \mathrm{cm}^{-3}$, which is not in conflict with the 3σ upper limit of $L_\mathrm{x} < 9 \times 10^{37}\ \mathrm{erg\,s}^{-1}$ (cf. Lewin et al. 1994). Quite recently, on day 1 368, another observation of SN 1994I provided a 3σ upper limit of $2.5 \times 10^{38}\ \mathrm{erg\,s}^{-1}$, which is much lower than expected for a constant velocity expansion into a constant density medium of $\rho = 2 \times 10^5\ \mathrm{cm}^{-3}$. Clearly, either the ambient density and/or the expansion speed are significantly lower at these later times and large distances.

Acknowledgements. We thank Kurt Weiler (NRL), Andy Read (MPE) and Andreas Vogler (MPE) for helpful discussions. The ROSAT project is supported by the German Bundesministerium für Bildung, Wissenschaft, Forschung und Technologie (BMBF/DARA) and the Max-Planck-Gesellschaft (MPG).

References

Baron, E., Hauschildt, P.H., Branch, D., et al., 1996, MNRAS 279, 799
Chandler, C.J., Phillips, J.A., Rupen, M.P., 1994, IAU Circ. No. 5978
Chevalier, R.A., 1984, ApJ 285, L63
Chevalier, R.A., Fransson, C., 1994, ApJ 420, 268
Chevalier, R.A., 1998, ApJ 499, 810
Clocchiatti, A., Brotherton, M., Harkness, R.P., et al., 1994, IAU Circ. No. 5972
Dickey, J.M., Lockman, F.J., 1990, ARA&A 28, 215
van Dyk, S.D., Weiler, K.W., Sramek, R.A., et al., 1993, ApJ 419, L69
Ehle, M., Pietsch, W., Beck, R., 1995, A&A 295, 289
Fabian, A.C., Terlevich, R., 1996, MNRAS 280, L5
Filippenko, A.V., Barth, A.J., Matheson, T., et al., 1995, ApJ 450, L11
Hasinger, G., Schmidt, M., Trümper, J., 1991, A&A 246, L2
Immler, S., Pietsch, W., Aschenbach, B., 1998a, A&A 331, 601
Immler, S., Pietsch, W., Ehle, M., et al., 1998b, in prep.
Irwin, M., Maddox, S., McMahon, R., 1994, Spectrum 2, 14
Lewin, W.H.G., Zimmermann, H.-U., Pietsch, W., et al., 1994, IAU Circ. No. 6019
Lewin, W.H.G., Zimmermann, H.-U., Aschenbach, B., 1996, IAU Circ. No. 6445
Nomoto, K., Yamaoka, H., Pols, O.R., et al., 1994, Nat 371, 227
Morrison, L.V., Argyle, R.W., 1994, IAU Circ. No. 5989
Puckett, T., Armstrong, J., Johnson, W., et al., 1994, IAU Circ. No. 5961
Raymond, J.C., Cox, D.P., Smith, B.W., 1976, ApJ 204, 290
Richmond, M.W., van Dyk, S.D., Ho, W., et al., 1996, AJ 111, 327
Rupen, M.P., Sramek, R.A., van Dyk, S.D., et al., 1994, IAU Circ. No. 5963
Schlegel, E.M., Petre, R., 1993, ApJ 412, L29
Schlegel, E.M., 1995, Rep. Prog. Phys. 58, 1375
Schmidt, B., Challis, P., Kirshner, R., et al., 1994, IAU Circ. No. 5966
Trümper, J., 1983, Adv. Space Res. 2, 241
Tully, R.B., 1988, 'Nearby Galaxies Catalog', Cambridge University Press
Vogler, A., Pietsch, W., 1996, A&A 311, 35
Weiler, K.W., van Dyk, S.D., Panagia, N., et al., 1993, Radio Supernovae & Massive Stellar Winds. In: Massive Stars: Their Lives in the Interstellar Medium, ASP Conf. Series, vol. 35, 436
Woosley, S.E., Langer, N., Weaver, T.A., 1995, ApJ 448, 315